

## IRAK-4 inhibitors. Part II: A structure-based assessment of imidazo[1,2-*a*]pyridine binding

George M. Buckley,<sup>a</sup> Thomas A. Ceska,<sup>b</sup> Joanne L. Fraser,<sup>a</sup> Lewis Gowers,<sup>a</sup> Colin R. Groom,<sup>a</sup> Alicia Perez Higuero,<sup>a,\*</sup> Kerry Jenkins,<sup>a,\*</sup> Stephen R. Mack,<sup>a</sup> Trevor Morgan,<sup>a</sup> David M. Parry,<sup>a</sup> William R. Pitt,<sup>a</sup> Oliver Rausch,<sup>a</sup> Marianna D. Richard<sup>a</sup> and Verity Sabin<sup>a</sup>

<sup>a</sup>UCB, Granta Park, Great Abington, Cambridge CB21 6GS, UK

<sup>b</sup>UCB, 216 Bath Road, Slough, Berkshire SL1 4EN, UK

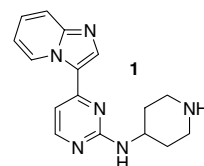
Received 12 March 2008; revised 15 April 2008; accepted 16 April 2008

Available online 22 April 2008

Dedicated to the memory of our friend and colleague David Rainey.

**Abstract**—A potent IRAK-4 inhibitor was identified through routine project cross screening. The binding mode was inferred using a combination of in silico docking into an IRAK-4 homology model, surrogate crystal structure analysis and chemical analogue SAR. © 2008 Elsevier Ltd. All rights reserved.

At UCB it is a routine practice to cross screen final compounds and advanced intermediates across kinase projects in early Discovery phase (Hit-to-Lead through to Lead Optimisation). Through this approach we identified compound **1**, from our JNK kinase programme,<sup>1</sup> which possessed significant potency in an IRAK-4 enzyme assay<sup>2</sup> but was poorly active against JNK-1 and JNK-2. There are many precedents for 2-aminopyrimidine-based kinase inhibitors, with this motif typically binding to the hinge backbone within the ATP-binding site.<sup>3</sup> This initially raised concerns over novelty and the potential for promiscuity associated with this scaffold. A close analogue example, **2**, from our JNK program exhibited this binding mode in a JNK-3 co-crystal structure (Fig. 1).<sup>4</sup> Attempts to crystallise IRAK constructs in-house were unsuccessful and there were no reported IRAK crystal structures in the public domain at this time.<sup>5</sup>



IRAK-4, IC<sub>50</sub> 216nM  
JNK-1, IC<sub>50</sub> 3801nM  
JNK-2, 59% inhib. @ 10μM

Some key analogues were prepared to explore the nature of the binding in IRAK-4 (Scheme 1). The ‘methyl capped’ compound, **4**, retained similar levels of potency to **1** suggesting that the bidentate HBA/HBD-binding mode was not responsible for activity. This was further supported by the O-linked pyrimidine, **5**, which despite lacking the aminopyrimidine-binding motif, still exhibited low-micromolar activity. The regioisomeric pyridines **6** and **7** showed contrasting SAR, with the 2,6-pyridine isomer **6** having low-nanomolar potency whilst the 2,4-pyridine isomer **7** showed little activity, despite having a more accessible bidentate-binding motif.

In the absence of an IRAK-4 crystal structure, a set of homology models were built using structural information from crystallographically elucidated kinases

**Keywords:** IRAK; IRAK-4; JNK; Kinase; Kinase inhibitor; IRAK-4 inhibitor; Homology model; Imidazopyridine; Imidazo[1,2-*a*]pyridine; Binding mode; JNK crystal structure; GASP; Docking; Hinge binder; Hinge region; Bidentate hydrogen bond; β-Turn; Protein modelling; IRAK-4 homology model; IRAK-4 crystal structure; Aminopyrimidine; Immunity; Anti-inflammatory; Hydrogen bond; P×G motif.

\* Corresponding authors. Tel.: +44 1223 896300; e-mail addresses: [alicia@cryst.bioc.cam.ac.uk](mailto:alicia@cryst.bioc.cam.ac.uk); [drkerryjenkins@yahoo.co.uk](mailto:drkerryjenkins@yahoo.co.uk)

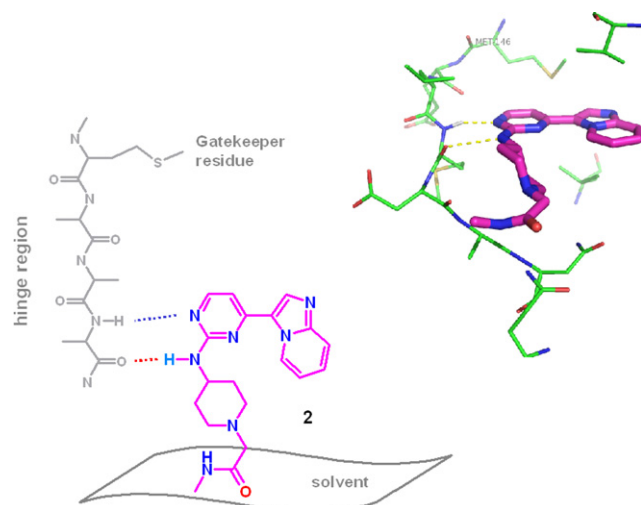


**Figure 1.** Structurally related aminopyrimidine **2** in JNK-3 crystal structure showing typical aminopyrimidine interaction with the hinge region (PDB code 3CGF).<sup>4</sup> IRAK-4 IC<sub>50</sub> 3  $\mu$ M, JNK-3 IC<sub>50</sub> 270 nM.

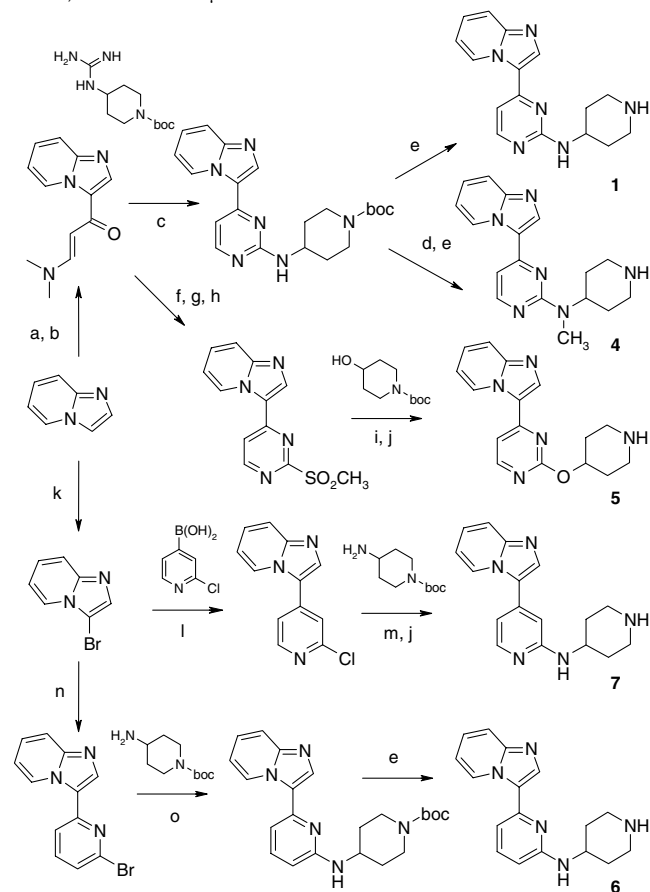
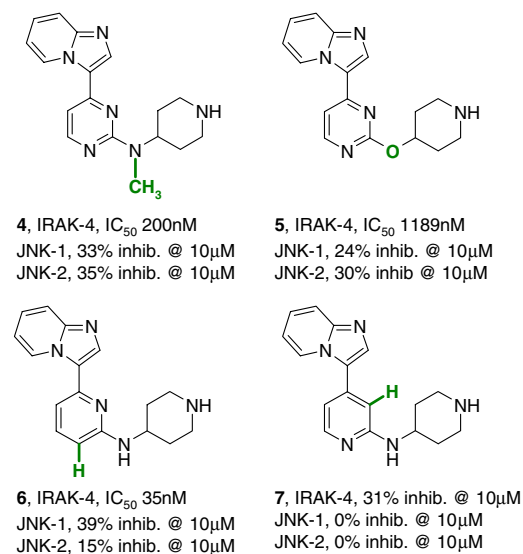
possessing similarity to IRAK-4 with respect to either the overall kinase domain or the ATP-binding site (for a more detailed discussion see the [Supplementary information](#)).

Docking the cross-screening hit **1** (see [Fig. 4](#) in [supplementary section](#)) into the IRAK-4 homology models suggested that the imidazopyridine nitrogen atom (N1) bound to the hinge backbone (Met265) and the aminopyrimidine moiety merely served as a linking scaffold rather than as the key binding feature. This binding mode was observed with a closely related 2-methylated aminopyrimidine analogue **8** (crystallised in JNK-3) that is incapable of forming the usual aminopyrimidine bidentate interaction ([Fig. 2](#)).<sup>6</sup>

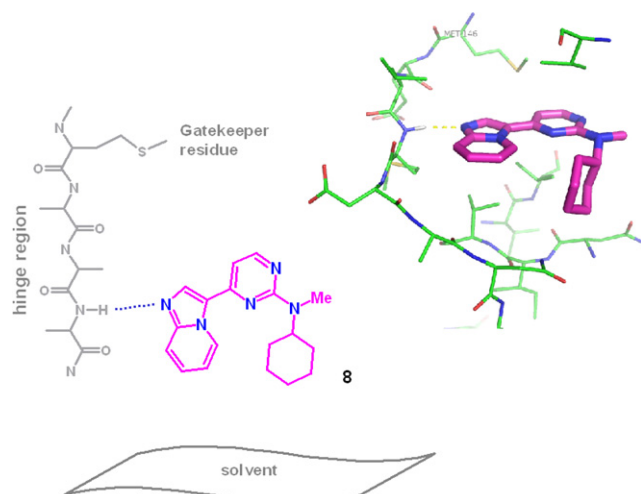
Pyridine **6** also docked favourably in this mode, adopting a ‘U-shaped’ conformation with the protonated piperidine ring nitrogen sitting in the anionic pocket formed by Asp329 and the carbonyl backbones of Asn316 and Ala315. Conformational analysis of the ligand showed that the docked binding conformation closely resembled its global minima conformation ([Fig. 3](#)).<sup>7</sup>

Docking experiments suggested that the poorly active compound **7** preferentially docked to the hinge region through the pyridine nitrogen ([Fig. 4](#)). Our homology model and subsequent crystal structure data<sup>5</sup> showed that the IRAK-4 hinge region does not have the 2nd carbonyl (Pro266) available to interact with the 2-amino group as it is engaged a type 1.  $\beta$ -Turn. Thus a bidentate HBD/HBA pairing was not a viable binding mode. In the ‘best docked’ mode the piperidine did not access the anionic pocket and the imidazopyridine experienced some notable close contacts.

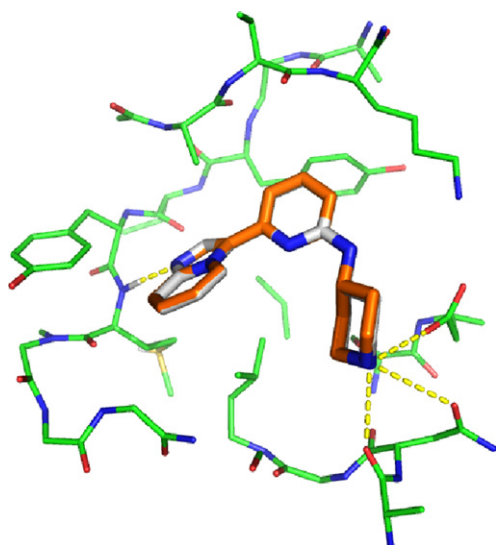
Conformational analysis revealed that compound **7** is more skewed than **6** in its low-energy conformations. This is most likely due to the steric differences arising from the regioisomeric pyridine methines interacting



**Scheme 1.** Synthesis of hit **1** and analogues **4–7**. Reagents and conditions: (a) AlCl<sub>3</sub>, 0 °C; Ac<sub>2</sub>O, 40 °C; (b) DMF–DMA, reflux (35%, two steps); (c) 1-Boc-4-guanidinopiperidine, NaH, DMF, reflux (60%); (d) NaH, DMF, rt, MeI, 60 °C (43%); (e) HCl, Et<sub>2</sub>O, DCM, MeOH (63–100%); (f) Thiourea, NaOMe, <sup>t</sup>BuOH, 150 °C, microwave; (g) MeI, <sup>t</sup>BuOH, (44%, two steps); (h) mCPBA, DCM, (77%); (i) 1-Boc-4-hydroxypiperidine, NaH, DMF, 80 °C (49%); (j) TFA, DCM (6–43%); (k) NBS, CHCl<sub>3</sub> (86%); (l) 2-Chloropyridyl-4-boronic acid, Pd(PPh<sub>3</sub>)<sub>4</sub>, Na<sub>2</sub>CO<sub>3</sub>, DME, H<sub>2</sub>O, 150 °C, microwave (13%); (m) 4-Amino-1-Boc piperidine, NaO<sup>t</sup>Bu, Pd(OAc)<sub>2</sub>, 1,3-bisdiphenylphosphinopropane, DME, 130 °C, microwave (28%); (n) <sup>t</sup>PrMgCl, THF, –78 °C; <sup>t</sup>Bu<sub>3</sub>SnCl, –78 °C–rt, 2,6-dibromopyridine, Pd(PPh<sub>3</sub>)<sub>4</sub>, rt–66 °C (75%); (o) 4-Amino-1-Boc piperidine, NaO<sup>t</sup>Bu, Pd(OAc)<sub>2</sub>, <sup>t</sup>Bu<sub>3</sub>PHBF<sub>4</sub>, DME, 85 °C (76%).



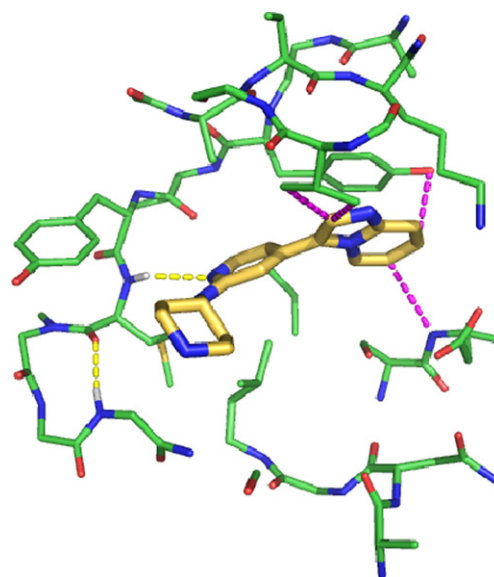
**Figure 2.** Structurally related aminopyrimidine **8** demonstrating alternative binding mode in JNK-3 crystal structure (PDB code: 3CGO).<sup>6</sup> IRAK-4 IC<sub>50</sub> 400 nM, JNK-3, IC<sub>50</sub> 3  $\mu$ M.



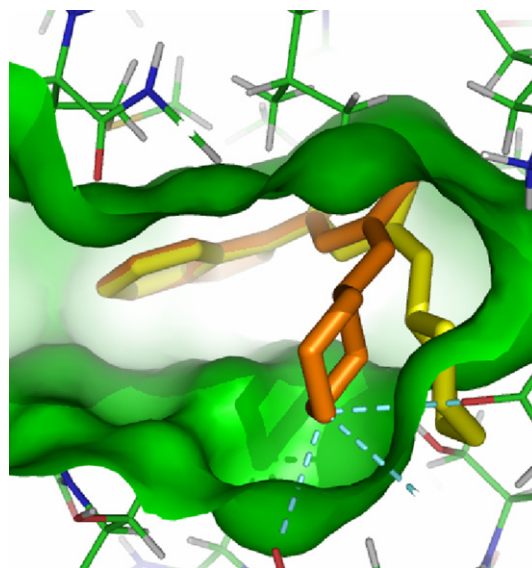
**Figure 3.** Docking mode of **6** (white) overlaid with the lowest energy conformation (orange). (Image generated with the program PyMol.)<sup>8</sup>

differently with both the imidazopyridine and aminopyridine rings. This distorts the conformation of **7** from the optimal 'U-shape' adopted by **6** and prevents the favourable positioning of the piperidine nitrogen into the anionic pocket. In this conformation the piperidine of **7** is likely to significantly clash with the protein active site surface. This can be seen from the overlay of **6** with **7** in its nearest local minima conformation (Fig. 5) and is a plausible explanation for the difference in potency seen between the two pyridine regioisomers.

These data encouraged us to pursue 2,6-pyridines as a discrete chemical series from the original pyrimidine hit. We then sought to further explore the role of the imidazo[1,2-*a*]pyridine motif (Table 1 and Scheme 2). Replacement of this bicycle with isoelectronic benzimidazole, **9**, gave rise to a potent IRAK-4 inhibitor whilst the approximately isosteric indole, **10**, only very weakly



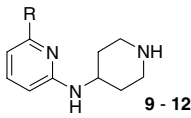
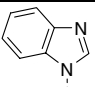
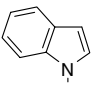
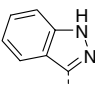
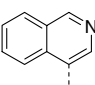
**Figure 4.** Suggested 'best docked' binding mode for **7**. Single hydrogen bond acceptor interaction through pyridine (yellow hashed line). Close contacts with imidazopyridine evident (magenta hashed lines).<sup>8</sup>

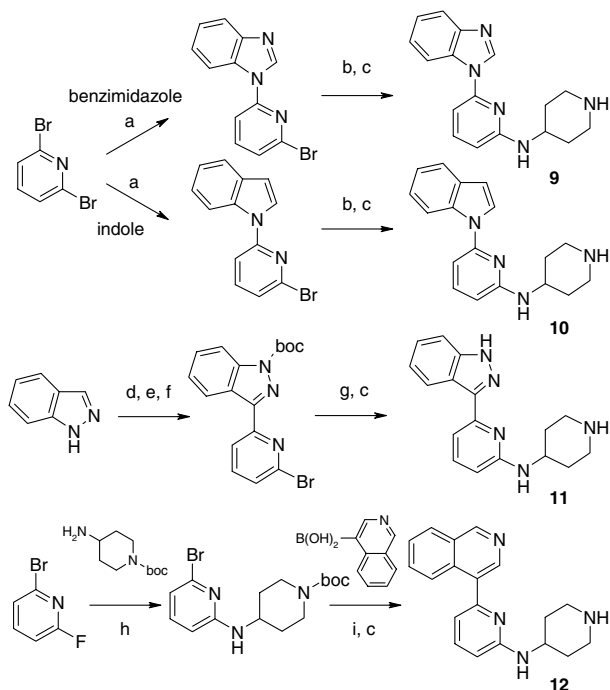


**Figure 5.** Docking mode of **6** (orange) overlaid with **7** (yellow) in its closest local minima to the 'U-shape' conformation.<sup>8</sup>

inhibited this enzyme. This further corroborated the significance of the hydrogen bond accepting nitrogen in this position in the bicyclic appendage. Interestingly, indazole **11** showed moderately good IRAK-4 potency. It is plausible that either nitrogen could act as a hydrogen bond acceptor through tautomerism, or alternatively this heterocycle might bind through a different mode altogether. Indeed it is noteworthy that compounds **9** and **10** exhibit little or no JNK potency whilst indazole **11** is modestly potent against JNK. This perhaps implicates the indazole in some alternative mode (or mixed modes) of binding. Isoquinoline **12** showed a significant but modest potency, possibly reflecting

**Table 1.** Alternative bicyclic heterocycles

 9–12		
Compound	R	IC <sub>50</sub> nM (or % inhibition at 10 μM)
9		IRAK-4, 70 nM JNK-1 (0%) JNK-2 (0%)
10		IRAK-4 (30%) JNK-1 (0%) JNK-2 (0%)
11		IRAK-4, 456 nM JNK-1, 2080 nM JNK-2, 1760 nM
12		IRAK-4, 1934 nM JNK-1 (5%) JNK-2 (0%)



**Scheme 2.** Synthesis of bicyclic replacement analogues, 9–12. Reagents and conditions: (a) NaH, indole or benzimidazole, NMP (33–75%); (b) 4-Amino-1-Boc piperidine, NaO<sup>t</sup>Bu, Pd(OAc)<sub>2</sub>, <sup>t</sup>Bu<sub>3</sub>PBHF<sub>4</sub>, DME, 120 °C, microwave (13–52%); (c) HCl, Et<sub>2</sub>O, DCM (27–70%); (d) I<sub>2</sub>, KOH, DMF, (90%); (e) <sup>t</sup>PrMgCl, THF, 0 °C; <sup>t</sup>Bu<sub>3</sub>SnCl, 0 °C–rt, 2,6-dibromopyridine, Pd(PPh<sub>3</sub>)<sub>4</sub>, rt–66 °C (64%); (f) Boc<sub>2</sub>O, Et<sub>3</sub>N, DMAP, MeCN (82%); (g) 4-Amino-1-Boc piperidine, Cs<sub>2</sub>CO<sub>3</sub>, Pd(OAc)<sub>2</sub>, <sup>t</sup>Bu<sub>3</sub>PBHF<sub>4</sub>, DME, 85 °C (47%); (h) 4-Amino-1-Boc piperidine, THF, 140 °C, microwave (50%); (i) Isoquinoline-4-boronic acid, Na<sub>2</sub>CO<sub>3</sub>, <sup>n</sup>Bu<sub>4</sub>NBr, Pd(PPh<sub>3</sub>)<sub>4</sub>, DME, H<sub>2</sub>O, reflux (40%).

the somewhat off-linear hydrogen bond interaction to Met265 seen in the best docked molecules (see Fig. 5 in the Supplementary section).

There are many approaches to hit finding, such as HTS/MTS of large screening decks against isolated targets, high content cell-based screening, ligand-based approaches (modification of natural ligands or known pharmacologically active compounds) and structure-based approaches (in silico screening, fragment screening by NMR or X-ray crystallography, de novo design). Here we have demonstrated the potential of project cross-fertilisation through routine cross screening of medicinal chemistry target compounds and advanced intermediates. This simple and pragmatic approach generated a new lead for our IRAK program. This fortuitous hit may have been overlooked from its perceived similarity to existing kinase inhibitors. However, the binding mode of the hit molecule was analysed in the absence of target crystallographic structural information using a combination of in silico modelling, synthetic analogues and surrogate kinase (JNK-3) crystallography. This gave us confidence that a novel binding mode was in operation and that the aminopyrimidine motif could be changed to a new and potentially more selective scaffold. The homology modelling helped to guide the lead optimisation and led to the generation of a highly potent series of IRAK-4 inhibitors with good drug-like properties and is the subject of another communication.<sup>9</sup> The validity of the IRAK homology models was subsequently corroborated by close overlay with published crystallographic data.<sup>5</sup>

### Acknowledgements

The authors extend their appreciation to the Analytical Sciences Department (for NMR, LC–MS and preparative HPLC), the enzyme assay and protein expression biologists and to the members of the JNK kinase project team.

### Supplementary data

Supplementary data associated with this article can be found, in the online version, at [doi:10.1016/j.bmcl.2008.04.039](https://doi.org/10.1016/j.bmcl.2008.04.039).

### References and notes

- (a) Alam, M.; Beevers, R. E.; Ceska, T.; Davenport, R. J.; Dickson, K. M.; Fortunato, M.; Gowers, L.; Haughan, A. F.; James, L. A.; Jones, M. A.; Kinsella, N.; Lowe, C.; Meissner, J. W. G.; Nicolas, A.-L.; Perry, B. G.; Phillips, D. J.; Pitt, W. R.; Platt, A.; Ratcliffe, A. J.; Sharpe, A.; Tait, L. *Bioorg. Med. Chem. Lett.* **2007**, *17*, 3463; (b) Ratcliffe, A. J.; World Patent WO038001, 2006.
- Buckley, G. M. et al. *Bioorg. Med. Chem. Lett.* **2008**, *18*, 3211.
- Some illustrative examples of aminopyrimidine kinase hinge binders include: (a) Bingham, A. H.; Davenport, R. J.; Gowers, L.; Knight, R. L.; Lowe, C.; Owen, D. A.; Parry, D. M.; Pitt, W. R. *Bioorg. Med. Chem. Lett.* **2004**, *19*, 409; (b) Sayle, K. L.; Bentley, J.; Boyle, F. T.; Calvert, A. H.; Cheng, Y.; Curtin, N. J.; Endicott, J. A.; Golding, B.

- T.; Hardcastle, I. R.; Jewsbury, P.; Mesguiche, V.; Newell, D. R.; Noble, M. E.; Parsons, R. J.; Pratt, D. J.; Wang, L. Z.; Griffin, R. J. *Bioorg. Med. Chem. Lett.* **2003**, *13*, 3079.
4. Coordinates submitted to the PDB: code 3CGF.
5. Since this work was carried out, researchers at Amgen (formerly Tularik) have published the first X-ray crystal structures of IRAK-4. Our homology model is in very close agreement to this structural data (see [Supplementary data](#)). Wang, Z.; Liu, J.; Sudom, A.; Ayres, M.; Li, S.; Wesche, H.; Powers, J. P.; Walker, N. P. C. *Structure* **2006**, *14*, 1835.
6. Coordinates submitted to the PDB: code 3CGO.
7. Conformational Searches were carried out with the program Sybyl (Tripos International, 1699 South Hanley Road, St. Louis, Missouri 63144, USA) using the grid search with 30° increment for both rotatable bonds (linker between Imidazopyridine–pyridine and between pyridine–amino group) with further minimisation for each conformer.
8. DeLano, W. L.; <http://www.pymol.org>.
9. Buckley, G. M. et al. *Bioorg. Med. Chem. Lett.* **2008**, doi:10.1016/j.bmcl.2008.04.042.